Journal of Bone Oncology 1 (2012) 40–46

Contents lists available at ScienceDirect

Journal of Bone Oncology

journal homepage: www.elsevier.com/locate/jbo

Research Article

Stathmin is involved in the cooperative effect of Zoledronic acid and gefitinib on bone homing breast cancer cells in vitro

Miki Oda [a,b], Keiichi Iwaya [b,*], Ryoko Kikuchi [b], Takayuki Kobayashi [b], Toshiyuki Yoneda [d], Kahoko Nishikawa [c], Osamu Matsubara [b], Norio Kohno [a]

[a] Department of Breast Oncology, Tokyo Medical University, Shinjuku, Tokyo, Japan
[b] Department of Basic Pathology, National Defense Medical College, 3-2 Namiki, Tokorozawa, Saitama 359-8513, Japan
[c] Department of Traumatology and Critical Care Medicine, National Defense Medical College, Tokorozawa, Saitama, Japan
[d] Department of Molecular and Cellular Biochemistry, Osaka University Graduate School of Dentistry, Suita, Osaka, Japan

ARTICLE INFO

Article history:
Received 27 April 2012
Received in revised form
12 June 2012
Accepted 12 June 2012
Available online 19 July 2012

Keywords:
Cell proliferation
Invasion
Bone-seeking clone
Two-dimensional fluorescence difference gel electrophoresis
Mass spectrometry

ABSTRACT

Zoledronic acid (Zol) is the most potent inhibitor of bone resorption among the bisphosphonates and is commonly used for inhibiting bone metastasis. However, it remains unclear whether Zol provides a survival benefit. Recent findings indicate that epidermal growth factor (EGF) signaling is an important mediator of bone metastasis. Thus, we examined the combined effects of Zol and an EGF receptor-tyrosine kinase inhibitor, gefitinib, on the proliferation and invasion of a bone-seeking clone and the breast cancer cell line MDA-MB-231. Combined treatment with Zol and gefitinib synergistically inhibited both invasion and cell proliferation of the bone-seeking clone, but not those of the MDA-MB-231 cells. Two-dimensional difference gel electrophoresis and mass spectrometry demonstrated that stathmin was down-regulated during these cooperative effects. Stathmin is a signal transduction regulatory factor which plays an important role in cell division and malignant tumor development. Our data suggest that stathmin may be a promising target molecule for blocking bone metastasis of breast cancer.

1. Introduction

Approximately 75% of patients with advanced breast cancer develop bone metastasis [1]. Patients with such bone metastasis suffer skeletal-related events (SREs) such as pathologic fracture, bone pain, spinal cord compression, and hypercalcemia [2]. As pathologic fracture is associated with a significantly increased risk of death, prevention of bone metastasis improves not only the quality of life but also the survival rate of patients with advanced breast cancer [3–5].

Zoledronic acid (Zol), which contains two nitrogen atoms within an imidazole ring structure, is the most potent inhibitor of bone metastasis-related osteolysis and effectively reduces the incidence of SREs [2]. Zol inhibits the mevalonate pathway in osteoclasts, thus inhibiting the synthesis of farnesyl pyrophosphate synthase and geranylgeranyl pyrophosphonate, which are required for prenylation of signaling GTPases. Recent preclinical studies have suggested that Zol exerts specific anti-tumor effects including inhibition of cancer cell proliferation and/or invasion [6–8].

Bisphosphonates significantly reduce or prevent SREs. The use of Zol for patients with bone metastases is currently the gold standard treatment [4]. However, it is still unclear whether Zol contributes to a survival benefit [9]. Niikura et al. recently reported that Zol did not prolong progression-free survival or overall survival of breast cancer patients with bone-only metastasis [10]. We aimed to enhance the anti-tumor effects on bone metastasis, epidermal growth factor receptor (EGFR)-tyrosin kinase inhibitor, gefitinib was used with Zol treatment.

Epidermal growth factor (EGF) signaling is also an important mediator of bone metastasis. The EGFR is overexpressed in a wide variety of cancer types including ~30% of breast cancers [11]. In addition to direct stimulation to cancer cell proliferation, EGF signaling has been implicated in the modulation of stromal cells in the tumor microenvironment [12,13]. Bone metastasis of the breast cancer clonal cell line MDA-MB-231, which overexpresses EGFR but lacks a proliferative response to EGF, is markedly suppressed by inhibition of EGFR-tyrosine kinase. In fact, significant relief of bone pain in breast cancer patients with bone metastases has been observed in a clinical trial of the EGFR-tyrosine kinase inhibitor gefitinib [14,15].

* Corresponding author at: Department of Basic Pathology, National Defense Medical College, 3-2 Namiki, Tokorozawa, Saitama 359-8513, Japan.
Tel.: +81 4 2995 2279; fax: +81 4 2996 5193.
E-mail address: kiwaya@ndmc.ac.jp (K. Iwaya).

2212-1374/$ - see front matter © 2012 Elsevier GmbH. This is an open access article under the CC BY-NC-ND license (http://creativecommons.org/licenses/by-nc-nd/4.0/).
http://dx.doi.org/10.1016/j.jbo.2012.06.001

We have studied a bone-seeking clonal cell line that was established by repeated sequential passages of metastatic cells from bone in nude mice and also in vitro, and shown that it metastasizes exclusively to bone, producing larger osteolytic lesions than the MDA-MB-231 parental cells. In contrast, MDA-MB-231 cells target other organs such as brain, ovary, liver, and adrenal gland. The biological properties of this bone-seeking clone were shown to differ from those of MDA-MB-231, the former producing more parathyroid hormone-released protein than the latter. Activation of insulin-like growth factor I occurred, and anchorage-independent growth was not inhibited by transforming growth factor β [16].

In the present study, we examined the combined effect of Zol and gefitinib on both cellular proliferation and invasion of the bone-seeking clone, in comparison with those of the parental MDA-MB-231 cells. The key protein responsible for the cooperative effects was identified by 2-dimensional fluorescence difference gel electrophoresis (2-D DIGE) and mass spectrometry.

2. Materials and methods

2.1. Cell cultures and drug treatment

The human breast cancer cell line MDA-MB-231 and its bone-seeking clone were studied. The bone-seeking clone had been established by repeated cardiac inoculation of the MDA-MB-231 parental cells into nude mice [16]. These cells were cultured in RPMI 1640 medium (Life Technologies Japan, Tokyo, Japan) supplemented with 10% fetal bovine serum (GE Healthcare Japan, Hino, Japan) and 1% penicillin (GE Healthcare Japan) at 37 °C under 5% CO_2.

Zol was provided by Novartis Pharma (Basel, Switzerland). Gefitinib (Iressa®) was purchased from Tocris Bioscience (St. Louis, MO, USA). Zol powder was dissolved in 0.1 N NaOH, and gefitinib powder was dissolved in dimethyl sulfoxide (DMSO). Cells were treated with 10 μM Zol and/or 1 μM gefitinib for 24 h or 72 h. The final concentration of NaOH or DMSO was less than 0.01% in all experiments.

2.2. Proliferation assay

Effects of Zol or gefitinib on cell proliferation were determined using the WST-8 assay (Dojindo, Kumamoto, Japan). This cell counting assay is sensitive for the determination of cell viability in cell proliferation assay. WST-8 is reduced by dehydrogenase activities in cells to give a yellow color formazan dye. The amount of formazan dye is directly proportional to the number of living cells. Brief protocol is as follows. Cells were seeded at a concentration of 1×10^4 cells per well in triplicate in a 96-well plate (Asahi Glass, Tokyo, Japan), and pre-incubated at 37 °C for 24 h to allow cell attachment. At 72 h after drug treatment, 10 μl of WST-8 solution was added to each well and incubated at 37 °C for 1 h. The assay is based on the extracellular reduction of WST-8 to a water-soluble formazan dye formed by NADH produced in mitochondria. The augmentation of enzyme activity leads to an increase in the amount of formazan dye, which was quantified using a microplate reader (BIOTEC, Tokyo, Japan) by measuring the absorbance at 450–550 nm. The above procedure was repeated at least three times.

2.3. Invasion assay

Invasion was estimated using a 24-well Boyden chamber (BD BioCoat™ Matrigel™ Invasion Chamber, BD Biosciences, San Jose, CA, USA) in accordance with the manufacturer's recommendations. After hydration of the matrigel inserts for 2 h, 5.0×10^4 cells in 500 μl RPMI medium containing 10 μM Zol, 1 μM gefitinib, or Zol plus gefitinib were added to the upper chambers. The lower chambers were filled with 750 μl RPMI medium containing drugs at the same concentrations as those in the upper chambers. After 24 h of incubation at 37 °C, non-invasive cells were removed from the membranes, and the membranes were fixed with methanol and stained with crystal violet. Only cells that had penetrated the membranes were counted in 10 randomly chosen high-power fields (HPFs) (× 400), and the mean number per HPF was adopted as the number of cells that had invaded through the membrane. The above experiments were performed in triplicate and repeated at least three times.

2.4. Protein extraction

The bone-seeking clone was cultured to 70% confluency and treated with each drug (Zol, gefitinib, or Zol plus gefitinib) for 24 h. The cells were then washed twice with ice-cold PBS, followed by fixation with 10% trichloroacetic acid, and scraped off into a tube and centrifuged at 3000 rpm for 10 min. The cell pellet was treated with lysis buffer (30 mM Tris, 2 M thiourea, 7 M urea, 4% CHAPS, dilute HCl, and dH_2O), and the resulting cell lysate was separated from debris by centrifugation and sonicated for 1.5 min at 250 W (Bioruptor, COSMO BIO, Yokohama, Japan). Protein concentration was measured with a 2-D Quant kit (GE Healthcare, Milwaukee, WI, USA).

2.5. 2-D DIGE (two-dimensional fluorescence difference gel electrophoresis)

Proteins were labeled with fluorescent cyanine dyes (GE Healthcare) in accordance with the manufacturer's instructions. In brief, 50 μg of a pair of samples extracted from the bone-seeking clone treated or untreated with an anti-cancer drug was adjusted to pH 8.5 with 50 mM NaOH and labeled with 400 pmol Cy3 or Cy5, while another pair of samples was labeled inversely with Cy5 or Cy3. The fluorescence labeling was performed on ice in the dark for 30 min, and then quenched with 1 μl of 10 mM lysine (Sigma–Aldrich, St. Louis, USA) for 10 min. Each preparation was treated with 2 × sample buffer containing 7 M urea, 2 M thiourea, 4% CHAPS,1% immobilized pH gradient (IPG)-buffer, pH range 4–7, and 2% dithiothreitol (DTT), and the final volume was adjusted to 260 μl with rehydration buffer (7 M urea, 2 M thiourea, 4% CHAPS, 0.5% IPG-buffer, pH range 4–7, 0.2% DTT). The proteins were applied to Immobiline DryStrips (pH 4–7, 13 cm) and focused on an Ettan IPGphor II (GE Healthcare).

Four focused IPG strips were equilibrated, and then loaded onto 12.5% SDS-polyacrylamide gels (30% acrylamide, 1.5 M Tris–HCl pH 8.8, 10% SDS, 10% APS, 10% TEMED) using low-fluorescence glass plates on an Ettan DALT II system (GE Healthcare). All electrophoresis procedures were performed in the dark. After SDS-PAGE, a pair of gels were scanned with a Typhoon 9410 scanner (GE Healthcare) with appropriate excitation/emission wavelengths specific for Cy3 (532/580 nm) and Cy5 (633/670 nm) to generate protein spot maps. The above procedure was repeated three times.

DeCyder 7.0 software (GE Healthcare) was used for 2-D DIGE analysis in accordance with the manufacturer's recommendation. The DeCyder differential in-gel analysis (DIA) module was used for pairwise comparisons of each sample. Differential protein spots ($|\text{ratio}| > 2$, $P < 0.05$) that showed consistent alteration were selected.

2.6. In-gel digestion and mass spectrometric analysis

Peptide mass fingerprinting (PMF) was performed for mass spectrometric analysis. To extract the differential protein spots,

500 μg of unlabeled sample was loaded onto SDS gel as described above. The gel was then stained with Coomassie blue for 1 h, and destained for 1 h in 10% acetic acid and 40% methanol. After washing with distilled water overnight, each spot was excised from the gel using a 1-ml pipet and kept in a PCR plate with water. In-gel digestion was performed as described by Kondo et al. [17]. Briefly, reduction was done using 45 mg DTT in 10 mM ammonium bicarbonate (ABM) and alkylation using 40 mg iodoacetamide in 50 mM ABM. After addition of 50% methanol, the gel plugs were washed in an ultrasonic water bath with ice for 10 min, then dehydrated with 50–100% acetonitrile (ACN) and incubated in vacuo for 10 min. Each procedure was performed 4–6 times. After drying for 1 h, the gel plugs were digested overnight in 0.5% trypsin in 50 mM ABM. The trypsin digests were recovered with 45% ACN and 0.1% trifluoroacetic acid (TFA), and the gel plugs were subjected to speedvac at room temp for 20 min. Finally, 15 μl of 0.1% TFA was added.

The trypsin digests were subjected to spiral mass spectrometry (JMS-S3000 MALDI-spiral TOF-TOF, Japan Electron Optics Laboratory, Akishima, Japan) and a database search was done using the Mascot search engine at http://www.matrix-science.com. Proteins that scored greater than 62 were judged to be significant ($P < 0.05$).

2.7. Western blot analysis

We further validated the identification of proteins using Western blot analysis. Samples from MDA-MB-231 cells and the derivative bone-seeking clone treated with 1 μM gefitinib and/or 100 μM Zol were extracted with cell lysis buffer (1 M Tris pH 7.5, NP-40, 5 M-NaCl, 0.5 M EDTA pH 7.5–8.0, 2 mM Na_3VO_4, 100 mM NaF, 10 mM NaP_2O_7). Fifty micrograms of each sample was separated using 12% SDS-PAGE gels, and transferred to a membrane using a Trans-Blot® Turbo™ Blotting System (Bio-Rad, Hercules, CA USA). After blocking with 5% non-fat milk powder in PBS overnight at 4 °C, the membranes were incubated with mouse monoclonal antibody against stathmin diluted 1:500 (BD Biosciences, San Jose, CA) or an anti-β-actin antibody (dilution 1:2000) (Sigma) for 1 h at room temperature. After washing with PBS containing 0.1% Tween 20, the membranes were incubated with the secondary antibody, anti-mouse IgG diluted at 1:2000 (GE Healthcare), for 30 min at room temperature and then washed for 30 min 4 times. The bands were reacted with chemiluminescence reagent (SuperSignal®, Thermo, Rockford, IL, USA) and visualized using a luminescence image analyzer (LAS-3000, Fuji Film, Kanagawa, Japan). The level of protein expression was evaluated using Multi Gauge ver. 3.0 (Fuji Film).

2.8. Statistical analysis

The significance of differences between the mean values of triplicate experiments in the proliferation and invasion assays was calculated using one-way analysis of variance (ANOVA) test. Differences were considered to be statistically significant at $P < 0.05$.

3. Results

3.1. Cell proliferation

Dose–response studies of Zol and gefitinib for both cell lines were shown in Figs. 1 and 2, respectively. Treatment with 10 μM Zol significantly reduced the absorbance of the bone-seeking clone from 0.77 nm (without any treatment) to 0.28 nm (reduction rate: 64%; 0.77–0.28/0.77; $P < 0.001$ indicated by *), and also that of MDA-MB-231 from 0.61 nm (without any treatment) to 0.17 nm (reduction rate: 72%; $P < 0.001$ indicated by **) (Fig. 3). In the bone-seeking clone, combined treatment with 10 μM Zol and 1 μM gefitinib reduced the absorbance by 50% to 0.14 nm, in comparison with a reduction to 0.28 nm by treatment with Zol alone ($P < 0.01$ indicated by ***). In contrast, the reduction rate

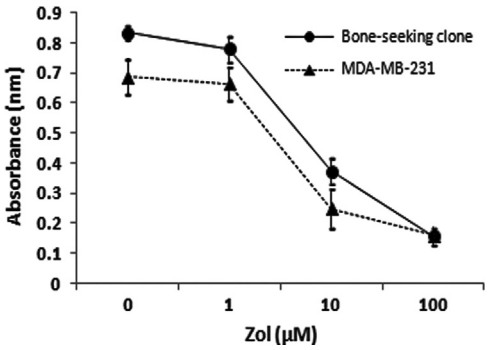

Fig. 1. Dose–response effects of Zol on cell proliferation of the bone-seeking clone and the MDA-MB-231 line. The cell counting WST-8 assay that is sensitive for the determination of cell viability was used. After 72 h of incubation, the formazan dye was quantified by absorbance at 450–550 nm. Each bar represents the standard error of the mean value from three replicates. Marked inhibitory effect was detected by the 10 μM Zol treatment.

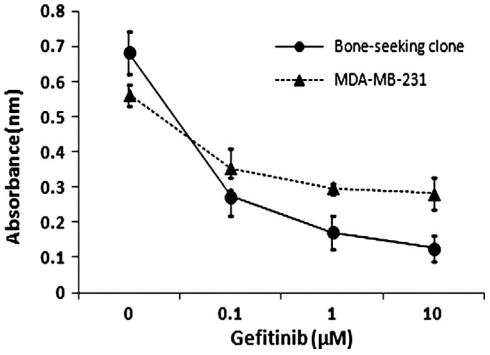

Fig. 2. Dose–response effects of gefitinib on cell proliferation of the bone-seeking clone and the MDA-MB-231 line. Cell viability was evaluated by the WST-8 assay. After 72 h of incubation, the formazan dye was quantified by absorbance at 450–550 nm. Each bar represents the standard error of the mean value from three replicates. Marked inhibitory effect was detected by the 1.0 μM gefitinib treatment.

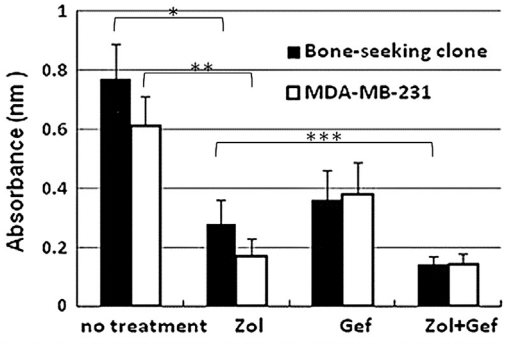

	no treatment	Zol	Gef	Zol+Gef
Bone-seeking clone	0.77 ± 0.12	0.28 ± 0.08	0.36 ± 0.10	0.14 ± 0.03
MDA-MB-231	0.61 ± 0.10	0.17 ± 0.06	0.38 ± 0.11	0.14 ± 0.04

Fig. 3. Effects of Zol and/or gefitinib on cell proliferation of the bone-seeking clone and the MDA-MB-231 line. Cells were treated with/without 10 μM Zol and/or 1.0 μM gefitinib (Gef). Zol treatment significantly inhibited proliferation of both the bone-seeking clone (*) and the MDA-MB-231 parental cells (**). An inhibitory effect of Zol plus Gef was detected on the bone-seeking clone ($P < 0.01$) (***), but not on MDA-MB-231. Each bar represents the standard error of the mean value.

was 18% in MDA-MB-231, and no significant cooperative effect of gefitinib with Zol was detected.

3.2. Invasion assay

The effects of Zol and/or gefitinib on invasion by the bone-seeking clone and MDA-MB-231 are shown in Fig. 4. The median number of cells that invaded through the membrane was significantly reduced by treatment with 10 μM Zol from 113.7 (without any treatment) to 35.0 (69%) for the bone-seeking clone ($P < 0.001$ indicated by *) and from 80.0 (without any treatment) to 36.7 (54%) for MDA-MB-231cells ($P < 0.05$ indicated by **). Combined treatment with 10 μM Zol plus 1 μM gefitinib markedly reduced the number of invading cells from 35.0 (treatment with Zol alone) to 4.3 (88%) for the bone-seeking clone ($P < 0.01$ indicated by ***), but no such significant effect was detected for MDA-MB-231 cells.

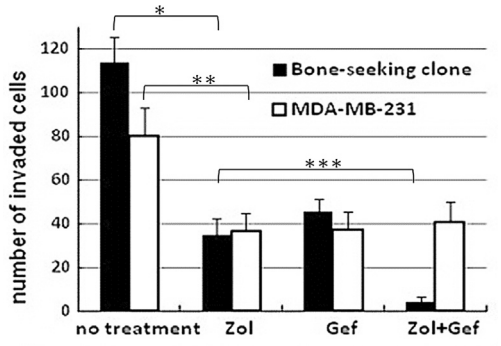

	no treatment	Zol	Gef	Zol+Gef
Bone-seeking clone	113.7 ± 11.5	35.0 ± 7.5	45.3 ± 5.8	4.3 ± 2.1
MDA-MB-231	80.0 ± 13.3	36.7 ± 8.0	37.0 ± 8.1	40.7 ± 9.5

Fig. 4. Effects of Zol and/or gefitinib on invasion of the bone-seeking clone and MDA-MB-231. A Boyden chamber was used to determine invasive ability. Cells were treated with/without 10 μM Zol and/or 1.0 μM Gef. After 24 h of incubation, non-invasive cells were removed from the membranes, and the membranes were stained with crystal violet. Only cells that had penetrated the membranes were counted in 10 HPFs (× 400) per filter. The mean number of invaded cells per HPF was adopted as the number of invaded cells. Zol treatment significantly decreased the number of invaded cells for both the bone-seeking clone (*) and MDA-MB-231(**). When the bone-seeking clone was treated with Zol plus Gef, a marked inhibitory effect on invasion was detected ($P < 0.01$) (***). However, no inhibitory effect was detected on MDA-MB-231 cells. Each bar represents the standard error of the mean value.

3.3. 2-D DIGE

2-D DIGE identified four spots whose expression levels were significantly changed by treatment with Zol (Fig. 5a). All four spots were up-regulated more than 3-fold. Treatment with 1.0 μM gefitinib alone induced differential up-regulation of the expression of one spot (indicated by the arrowhead in Fig. 5c and d), but the other spots showed no significant change in expression though many spots were differentially expressed within 2-folds up- or down-regulation.

When the bone-seeking clone was treated with both Zol and gefitinib, these four spots were confirmed to show a change in protein level. Moreover, three new spots, numbered ①～③, appeared and showed significant down-regulation of their expression (Fig. 5d). These three spots, whose expression levels were not changed by treatment with either Zol or Gef alone (Fig. 5b and c, respectively), were located within a pH range of 5–6 and had molecular masses of 17–20 kDa. They were then subjected to identification by mass spectrometry.

3.4. Mass spectrometric analysis

We focused on the three protein spots (Fig. 5b–d ①～③) whose expression was significantly down-regulated by combined treatment with the two drugs. Fig. 6 shows the peak flow of the digested peptide derived from spot ③, which was identified as stathmin by a Mascot search. Among the three spots, ② and ③ shared a common sequence of 16 peptides ($P = 0.005$). There was no evident difference in the amino acid sequences that could

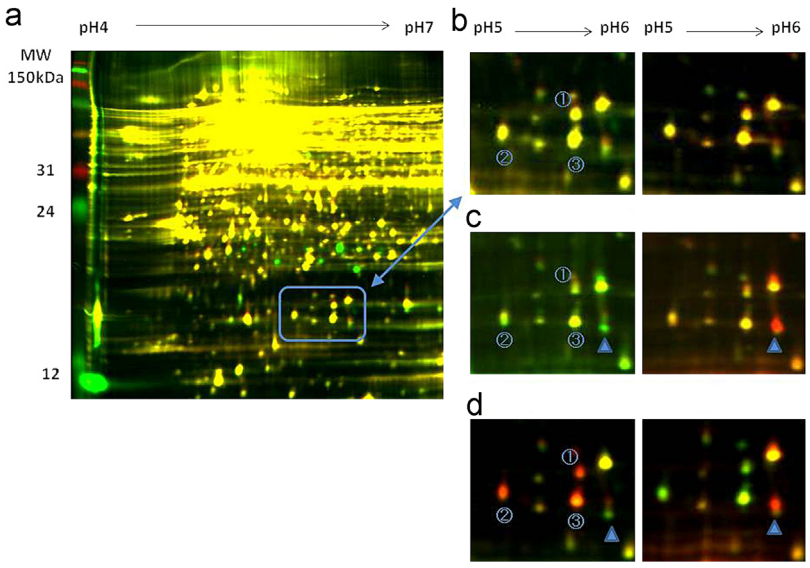

Fig. 5. Changes in the profile of spots detected by 2-D DIGE in the bone-seeking clone. (a) When the protein lysate after treatment with Zol was labeled with cy3, spots with increased expression were visualized as green spots. Four spots were up-regulated more than 3-fold. The majority of merged spots that showed no change in expression level were visualized as yellow. (b) High-magnification view of the area corresponding to pH 5–6, 17–20 kDa, indicated by the blue rectangle in Fig. 5a. Three yellow spots numbered by ①–③ are shown. (c) The expression levels of these three spots were not changed by treatment with Gef. (d) These three spots were down-regulated (red spots) by combined treatment with Zol and Gef. Conversely, when the proteins after treatment with both drugs were labeled with cy5, the down-regulated spots were confirmed to be visualized as green. (For interpretation of the references to colour in this figure legend, the reader is referred to the web version of this article.)

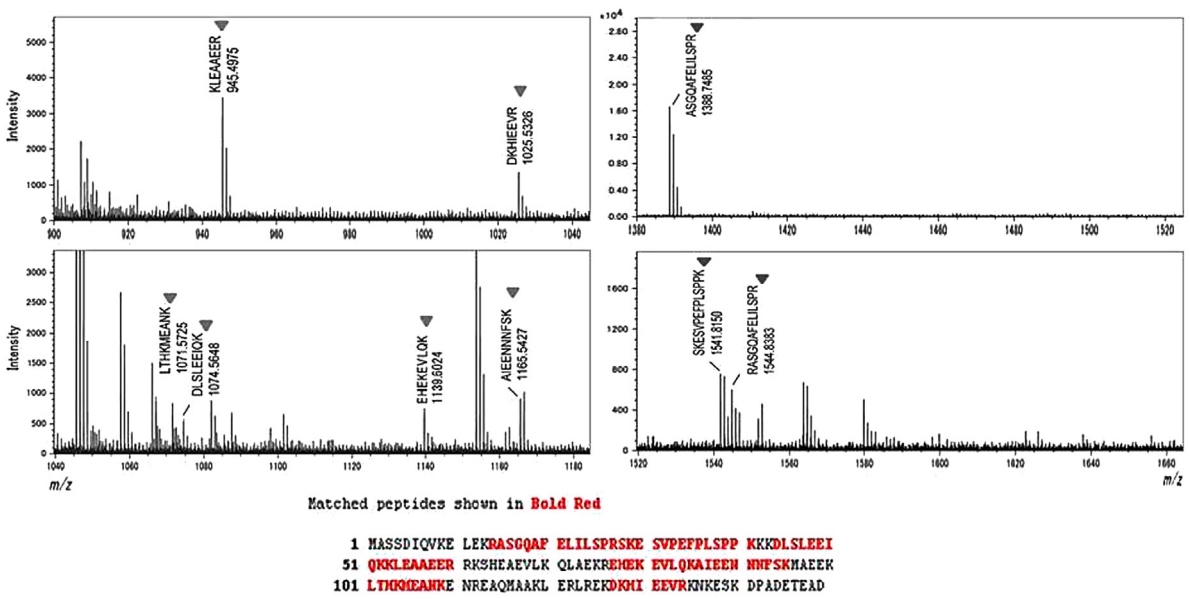

Fig. 6. Peptide map derived from spots ② and ③ and amino acid sequence determined by mass spectrometry. Each spot was excised from the gel, and in-gel digestion was performed. The trypsin digests were subjected to spiral mass spectrometry, and a database search was performed using the Mascot software. Each peak of matched peptides indicated by arrow head is appended by mass-to-charge ratio and amino acid sequence. Spots ② and ③ showed almost the same sequence and were identified as stathmin.

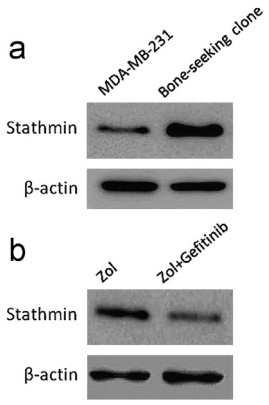

Fig. 7. Expression of stathmin determined by Western blot analysis. Samples with equal amounts (50 μg) of cell lysates from the bone-seeking clone and MDA-MB-231 were separated by 12% SDS-PAGE, transferred to membranes, and incubated with the anti-stathmin monoclonal antibody. β-Actin was used as a positive control. (a) Stathmin was expressed in the bone-seeking clone at a higher level than in MDA-MB-231. (b) Stathmin was down-regulated by combined treatment with Zol and Gef in the bone-seeking clone in comparison with Zol treatment alone.

explain their different electrophoretic mobilities. Spot ① could not be identified in this study.

3.5. *Western blot analysis*

Expression of stathmin in the bone-seeking clone was increased 6-fold in comparison with that in the parental line, MDA-MB-231 (Fig. 7a). In the bone-seeking clone, it was confirmed that the expression level of stathmin was halved by combined treatment with Zol and gefitinib, in comparison with Zol alone (Fig. 7b). This kind of down-regulation was not clearly detected in MDA-MB-231 because MDA-MB-231 expressed stathmin lower than bone-seeking clone without the treatment of Zol or gefitinib. (data not shown).

4. Discussion

Zol acts against osteolytic bone metastasis by inducing isoprenylation of proteins that are required for osteoclast survival. It also induces apoptosis in several types of cancers, including primary breast cancer, through the pathway responsible for prenylation of small GTP-binding proteins [18]. It is well known that EGF is an anti-apoptotic factor, and it is conceivable that gefitinib might enhance the susceptibility of cancer cells to apoptosis. In fact, a combination of Zol and gefitinib with SC-234 was reported to elicit a cooperative anti-tumor effect in a non-bone metastatic model of breast and prostate cancer [19]. Such combined treatment has also been reported to elicit a tumor-suppressive effect, which is significantly more effective and less toxic in vitro and in vivo, on EGFR-mutated non-small cell lung carcinoma cells, in comparison with the individual anti-tumor effect of gefitinib or Zol alone [20]. In the present study using a bone-seeking breast cancer clonal cell line in vitro, we demonstrated an enhanced inhibitory effect on bone metastasis using Zol plus gefitinib in combination.

The bone-seeking clone used in this study showed higher expression of stathmin than the parental MDA-MB-231 cell line. Similarly, using 2-D DIGE and mass spectrometry, Xu et al. have demonstrated that stathmin-1 was up-regulated in a highly metastatic variant of MDA-MB-231 [21]. A proteomic analysis designed to examine the time course of neoplastic transformation of human mammary epithelial cells showed that stathmin was up-regulated in parallel with an early and progressive increase in metastatic potential [22]. Moreover, overexpression of stathmin has been detected in different types of human malignant tissue, such as sarcoma [23], gastric cancer [24], endometrial cancer [25], colon cancer [26], nasopharyngeal cancer [27], and breast cancer [28,29]. All these data suggest that overexpression of stathmin is significantly correlated with clinically aggressive behavior such as lymph node metastasis, poor histologic differentiation, an advanced clinical stage, or poor prognosis.

In the present study, we found that stathmin was significantly down-regulated upon treatment with a combination of Zol and gefitinib. The down-regulation of stathmin, which was not detected by 2-D DIGE after treatment with either agent alone,

was considered to be attributable to cooperative effect of Zol and gefitinib. Down-regulation of endogenous stathmin by transfection with an adenovirus expressing stathmin small interfering RNA (siRNA) was reported to decrease the migration of HT1080 (human fibrosarcoma) cells through fibronectin-coated Transwells [23]. Silencing of stathmin by siRNA has also been shown to decrease the proliferation, viability, or invasion of cancer cells derived from malignancies of the prostate [30], breast [31], stomach [24], and colon [26]. These findings are in accord with our present data indicating that down-regulation of stathmin paralleled the inhibition of both cell proliferation and invasion of the bone-seeking clone upon combined treatment with Zol and gefitinib, suggesting that stathmin could be a potential candidate for therapeutic target for inhibition of bone metastasis.

Finally, our data allow us to propose a potentially promising strategy for cancer therapy. Down-regulation of stathmin has been reported to enhance the sensitivity to anti-microtubule drugs [32–34]. Because the combined treatment of Zol and gefitinib down-regulates the expression of stathmin, a further inhibitory effect against breast cancer might be expected if anti-microtubule drugs were to be added. Although a preclinical study would be needed to investigate this triple strategy, synergistic anti-angiogenic effects of stathmin inhibition and taxol exposure have already been reported [35]. Combination of these three agents might be indicated for patients with aggressive breast cancers such as those with the triple negative phenotype.

In summary, we have demonstrated that combined treatment with Zol and gefitinib, which down-regulate stathmin, produces enhanced anti-tumor effects on bone homing breast cancer cells in vitro. Thus, co-administration of Zol and gefitinib may constitute a basis for developing a more effective therapy for patients with bone metastasis.

Acknowledgments

We are grateful to Mr. Masahiro Hashimoto and Mr. Yoshiyuki Itoh, Japan Electron Optics Laboratory (JEOL) Co., Ltd., Akishima, Tokyo, Japan, for providing the data of mass spectrometric analysis, and Ms. Kozue Suzuki for skilled assistance with protein labeling and loading for 2D-DIGE. This study was supported in part by the Foundation for Promotion of Cancer Research, a Ministry of Defense Grant (Osamu Matsubara and Keiichi Iwaya), by a Grant-in-aid for Scientific Research (C) (KAKENHI24590457) and by the National Cancer Center Research and Development Fund (23-A-11).

References

[1] Coleman RE. Metastatic bone disease: clinical features, pathophysiology and treatment strategies. Cancer Treatment Reviews 2001;27:165–76.
[2] Neville HL, Coleman RE. Bisphosphonates and RANK ligand inhibitors for the treatment and prevention of metastatic bone disease. European Journal of Cancer 2010;46:1211–22.
[3] Saad F, Lipton A, Cook R, Chen YM, Smith M, Coleman R. Pathologic fractures correlate with reduced survival in patients with malignant bone disease. Cancer 2007;110:1860–7.
[4] Kohno N, Aogi K, Minami H, Nakamura S, Asaga T, Takashima S, et al. Zoledronic acid significantly reduces skeletal complications compared with placebo in Japanese women with bone metastases from breast cancer: a randomized, placebo-controlled trial. Journal of Clinical Oncology 2005; 23:3314–21.
[5] Coleman R, Brown J, Terpos E, Lipton A, Smith MR, Major P, et al. Bone markers and their prognostic value in metastatic bone disease: clinical evidence and future directions. Cancer Treatment Reviews 2008;34: 629–39.
[6] Boissier S, Ferreras M, Peyruchaud O, Magnetto S, Ebetino FH, Clezardin P, et al. Bisphosphonates inhibit breast and prostate carcinoma cell invasion, an early event in the formation of bone metastases. Cancer Research 2000; 60:2949–54.
[7] Denoyelle C, Hong L, Vannier J-P, Soria J, Soria C. New insights into the actions of bisphosphonate Zoledronic acid in breast cancer cells by dual RhoA-dependent and -independent effects. British Journal of Cancer 2003; 88:1631–40.
[8] Almubarak H, Jones A, Chaisuparat R, Zhang M, Meiller TF, Scheper MA. Zoledronic acid directly suppresses cell proliferation and induces apoptosis in highly tumorigenic prostate and breast cancers. Journal of Carcinogenesis 2011;10:1–10.
[9] Coleman RE, Marshall H, Cameron D, Dodwell D, Burkinshaw R, Bell R, et al. Breast-cancer adjuvant therapy with Zoledronic acid. New England Journal of Medicine 2011;365:1396–405.
[10] Niikura N, Liu J, Hayashi N, Palla SL, Tokuda Y, Theriault RL. Retrospective analysis of antitumor effects of Zoledronic acid in breast cancer patients with bone-only metastases. Cancer 2011:1–9.
[11] Irwin ME, Mueller KL, Bohin N, Ge Y, Boerner JL. Lipid raft localization of EGFR alters the response of cancer cells to the EGFR tyrosine kinase inhibitor gefitinib. Journal of Cellular Physiology 2011;226:2316–28.
[12] Lu X, Wang Q, Hu G, Poznak CV, Fleisher M, Kang Y, et al. ADAMTS1 and MMP1 proteolytically engage EGF-like ligands in an osteolytic signaling cascade for bone metastasis. Genes & Development 2009;23:1882–94.
[13] Lu X, Kang Y. Epidermal growth factor signaling and bone metastasis. British Journal of Cancer 2010;102:457–61.
[14] Albain K, Elledge R, Gradishar WJ, Hayes DF, Rowinsky E, Pusztai L, et al. Open-label, phase II, multicenter trial of ZD1839 ('Iressa') in patients with advanced breast cancer. Breast Cancer Research and Treatment 2002;76:20 abstract.
[15] Von MG, Jonat W, Beckmann M, De BA, Kleeberg U, Schneeweiss A, et al. A multicenter phase II trial to evaluate gefitinib ('Iressa', ZD1839)(500 mg/d) in patients with metastatic breast cancer after previous chemotherapy treatment. European Journal of Cancer 2003;1:S133 abstract.
[16] Yoneda T, Williams PJ, Hiraga T, Niewolna M, Nishimura R. A bone-seeking clone exhibits different biological properties from the MDA-MB-231 parental human breast cancer cells and a brain-seeking clone in vivo and in vitro. Journal of Bone and Mineral Research 2001;16:1486–95.
[17] Kondo T, Hirohashi S. Application of highly sensitive fluorescent dyes (CyDye DIGE Fluor saturation dyes) to laser microdissection and two-dimensional difference gel electrophoresis (2D-DIGE) for cancer proteomics. Nature Protocols 2006;1:2940–50.
[18] Caraglia M, D'Alessandro AM, Marra M, Giuberti G, Vitale G, Abbruzzese A, et al. The farnesyl transferase inhibitor R115777 (Zarnestra®) synergistically enhances growth inhibition and apoptosis induced on epidermoid cancer cells by Zoledronic acid (Zometa®) and pamidronate. Oncogene 2004;23: 6900–13.
[19] Melisi D, Caputo R, Damiano V, Bianco R, Veneziani BM, Tortora G, et al. Zoledronic acid cooperates with a cyclooxygenase-2 inhibitor and gefitinib in inhibiting breast and prostate cancer. Endocrine-Related Cancer 2005;12: 1051–8.
[20] Chang JW, Hsieh JJ, Shen YC, Yeh KY, Wang CH, Hsu T, et al. Bisphosphonate Zoledronic acid enhances the inhibitory effects of gefitinib on EGFR-mutated non-small cell lung carcinoma cells. Cancer Letters 2009;278:17–26.
[21] Xu SG, Yan PJ, Shao ZM. Differential proteomic analysis of a highly metastatic variant of human breast cancer cells using two-dimensional differential gel electrophoresis. Journal of Cancer Research and Clinical Oncology 2010;136:1545–56.
[22] DeAngelis JT, Li Y, Mitchell N, Wilson L, Kim H, Tollefsbol TO. 2D difference gel electrophoresis analysis of different time points during the course of neoplastic transformation of human mammary epithelial cells. Journal of Proteome Research 2010;447:447–58.
[23] Belletti B, Nicoloso MS, Schiappacassi M, Berton S, Lovat F, Baldassarre G, et al. Stathmin activity influences sarcoma cell shape, motility, and metastatic potential. Molecular Biology of the Cell 2008;19:2003–13.
[24] Jeon TY, Han ME, Lee YW, Lee YS, Kim GH, Oh SO, et al. Overexpression of stathmin 1 in the diffuse type of gastric cancer and its roles in proliferation and migration of gastric cancer cells. British Journal of Cancer 2010;102: 710–8.
[25] Trovik J, Wik E, Stefansson IM, Marcickiewicz J, Tingulstad S, Salvesen HB, et al. Stathmin overexpression identifies high-risk patients and lymph node metastasis in endometrial cancer. Clinical Cancer Research 2011;17: 3368–77.
[26] Zheng P, Liu YX, Chen L, Liu XH, Xiao ZQ, Zhao L, et al. Stathmin, a new target of PRL-3 identified by proteomic methods, plays a key role in progression and metastasis of colorectal cancer. Journal of Proteome Research 2010;9: 4897–905.
[27] Cheng AL, Huang WG, Chen ZC, Peng F, Zhang PF, Xiao ZQ. Identification of novel nasopharyngeal carcinoma biomarkers by laser capture microdissection and proteomic analysis. Clinical Cancer Research 2008;14:435–45.
[28] Brattsand G. Correlation of oncoprotein 18/stathmin expression in human breast cancer with established prognostic factors. British Journal of Cancer 2000;83:311–8.
[29] Curmi PA, Nogues C, Lachkar S, Carelle N, Gonthier MP, Bieche I, et al. Overexpression of stathmin in breast carcinomas points out to highly proliferative tumours. British Journal of Cancer 2000;82:142–50.
[30] Mistry SJ, Bank A, Atweh GF. Targeting stathmin in prostate cancer. Molecular Cancer Therapeutics 2005;4:1821–9.

[31] Alli E, Yang JM, Hait WN. Silencing of stathmin induces tumor-suppressor function in breast cancer cell lines harboring mutant p53. Oncogene 2007;26:1003–12.
[32] Wang R, Dong K, Lin F, Wang X, Gao P, Wei SH, et al. Inhibiting proliferation and enhancing chemosensitivity to taxanes in osteosarcoma cells by RNA interference-mediated downregulation of stathmin expression. Molecular Medicine 2007;13:567–75.
[33] Long M, Yin G, Liu L, Lin F, Wang X, Ren J, et al. Adenovirus-mediated Aurora A shRNA driven by stathmin promoter suppressed tumor growth and enhanced paclitaxel chemotherapy sensitivity in human breast carcinoma cells. Cancer Gene Therapy 2012;19:271–81.
[34] Alli E, Babula JB, Yang JM, Hait WN. Effect of stathmin on the sensitivity to antimicrotubule drugs in human breast cancer. Cancer Research 2002;62: 6864–9.
[35] Mistry SJ, Bank A, Atweh GF. Synergistic antiangiogenic effects of stathmin inhibition and taxol exposure. Molecular Cancer Research 2007;5:773–82.